J. Plasma Phys. (2023), *vol*. 89, 905890107
Published by Cambridge University Press
doi:10.1017/S0022377822001313

Terahertz radiation in the interaction of a focused laser pulse with plasma

A.A. Frolov †

Lebedev Physical Institute, Russian Academy of Sciences, Moscow 119991, Russia

(Received 2 November 2022; revised 22 December 2022; accepted 22 December 2022)

The theory of terahertz (THz) wave emission at the oblique incidence of a focused *s*-polarized laser pulse on the boundary of a rarefied plasma is developed. The angular, spectral and energy characteristics of the THz signal as a function of the focal spot size and the incidence angle of laser radiation, as well as the plasma density, are investigated. It is shown that the THz radiation energy increases with a decrease in the laser pulse focal spot and has the maximum value when the tightly focused laser pulse is incident at the angle of total reflection on the plasma boundary.

Key words: plasma nonlinear phenomena

1. Introduction

The current interest in terahertz (THz) radiation and the mechanisms of its generation is associated with the possibilities of its use in science, technology, medicine and other practical applications (Song & Nagatsuma 2015). In recent times, laser radiation interacting with various material media has been widely used to generate high-power pulses of THz radiation. For the first time, THz pulses under laser irradiation of gas and solid-state targets were detected in an experiment (Hamster *et al.* 1993). Subsequently, THz radiation was recorded in many experiments under laser action on gases (Yugami *et al.* 2002; Dorranian *et al.* 2003; Schroeder *et al.* 2004; Sprangle *et al.* 2004; van Tilborg *et al.* 2006; Gopal *et al.* 2013), solids (Weiss, Wallenstein & Beigang 2000; Kadlec, Kuzel & Coutaz 2004, 2005; Welsh & Wynne 2009; Suvorov *et al.* 2012) and clusters (Nagashima *et al.* 2009; Jahangiri *et al.* 2011; Oh *et al.* 2013). At present, the most intense THz radiation with a high conversion rate has been experimentally detected at the laser irradiation of lithium niobate crystals (Huang *et al.* 2013; Fülöp *et al.* 2014) and organic crystals (Vicario *et al.* 2014, 2015).

Various mechanisms of THz wave emission under laser action have been theoretically considered for rarefied plasma (Gorbunov & Frolov 1996; Yoshii *et al.* 1997; Gorbunov & Frolov 2004; Sheng *et al.* 2005; Gorbunov & Frolov 2006; Dong *et al.* 2009; Dechard *et al.* 2018; Liao & Li 2019), for dense plasma and conductors (Frolov 2007; Urupin & Frolov 2012; Dechard *et al.* 2020) and for clusters (Frolov 2018). The important theoretical problem is to increase the energy of the THz pulse and the conversion rate in the interaction of laser radiation with matter. Recently, it was shown in Frolov (2020, 2021) that, if laser radiation is incident at the angle of total reflection on the boundary of a

† Email address for correspondence: frolovaa@lebedev.ru

subcritical plasma, then the energy of the generated THz pulse increases by more than an order of magnitude. At the same time, in Frolov (2020, 2021), the problem of the incidence of unfocused *s*- and *p*-polarized laser radiation on a plasma was considered. In this article, in contrast to Frolov (2020), we consider the emission of THz waves from plasma for incident focused *s*-polarized laser radiation. It is shown that the energy of the THz signal increases significantly with a decrease in the size of the laser radiation focal spot and is maximum when the tightly focused laser pulse is incident at the angle of total reflection on the plasma boundary. Let us recall that, for *s*-polarized electromagnetic radiation, the electric field vector is perpendicular to the plane of incidence (i.e. the plane in which the wave vectors of the incident and reflected waves lie), and the magnetic field of this radiation lies in the plane of incidence. In the case of a *p*-polarized wave, the electric field vector lies in the plane of incidence and the magnetic field is perpendicular to this plane.

This article has the following structure: in § 2, we consider the boundary value problem for a focused *s*-polarized laser pulse when it falls on the plasma boundary, the electron density of which is much less than the critical value. The electric field and ponderomotive potential of laser radiation in plasma near the plasma–vacuum interface are calculated. It is shown that the grazing incidence of the laser pulse at the angle of total reflection leads to an increase in the ponderomotive potential by a factor of 4 compared with the incidence at smaller angles. In § 3, based on Maxwell's equations averaged over high-frequency laser oscillations and the equation of motion for plasma electrons, taking into account the ponderomotive action of laser radiation, the excitation of THz fields in plasma and in vacuum is considered. The emission of THz waves from plasma into vacuum is considered in § 4, where the angular, spectral and energy characteristics of the THz signal are studied as functions of the incidence angle and the focusing degree of laser radiation, as well as the plasma density. It is shown that the energy of the THz signal increases with a decrease in the size of the laser radiation focal spot and has the maximum value at the grazing incidence of the tightly focused laser pulse at the angle of total reflection onto the rarefied plasma boundary. In the Conclusion, the main results of the article are presented and estimates are given for the characteristics of THz radiation under the conditions of modern laser-plasma experiments.

2. Boundary value problem for laser radiation

Let an *s*-polarized laser pulse with the carrier frequency ω_0 and the time duration τ significantly exceeding the oscillation period ($\tau \gg 1/\omega_0$) be incident on the plasma, which occupies the region of space $z > 0$, from vacuum ($z < 0$) at the angle α with respect to the normal to the plasma–vacuum interface. We assume that the size of the pulse in the direction of the *y*-axis significantly exceeds its size along the *x* and *z* axes. Then the electric field of the incident Gaussian laser radiation in vacuum ($z < 0$) near the plasma boundary ($|z| \ll k_0 R_x^2$) can be represented in the following form:

$$\boldsymbol{E}_L^{\mathrm{inc}}(\boldsymbol{r}, t) = \frac{1}{2}\boldsymbol{e}_y E_{0L} \exp\left\{-\mathrm{i}\omega_0\left(t - \frac{z'}{c}\right) - \frac{1}{2\tau^2}\left(t - \frac{z'}{c}\right)^2 - \frac{x'^2}{2R_x^2}\right\} + \mathrm{c.c.}, \qquad (2.1)$$

where E_{0L} is the amplitude of the laser field, $z' = z\cos\alpha + x\sin\alpha$ is the axis characterizing the direction along which the incident pulse propagates, the axis $x' = x\cos\alpha - z\sin\alpha$ is perpendicular to the z' axis, $\boldsymbol{e}_y$ is the basis vector of the y axis in the Cartesian coordinate system, R_x is the transverse size of the laser pulse (along the x' axis), which we will consider to be much larger than the wavelength of laser radiation $\lambda_0 = 2\pi c/\omega_0$, $k_0 = \omega_0/c$ is the wavenumber, $L = c\tau$ is the longitudinal size of the laser pulse, c is the speed of light and c.c. is the complex conjugate.

https://doi.org/10.1017/S0022377822001313 Published online by Cambridge University Press

This configuration of the focal spot in the form of a line at the plasma boundary takes place when laser radiation is focused by a cylindrical lens. We will assume that the frequency of laser radiation ω_0 significantly exceeds the plasma frequency $\omega_p = \sqrt{4\pi e^2 N_{0e}/m_e}$, this condition corresponds to a rarefied plasma with the electron density N_{0e} that is significantly less than the critical value $N_{\rm cr} = m_e\omega_0^2/(4\pi e^2)$, that is, the inequalities $\omega_0 \gg \omega_p$, $N_{0e} \ll N_{\rm cr}$ are satisfied, where e, m_e are the charge and mass of the electron. Using a Fourier transform with respect to time and x coordinate, we write the total field of the laser radiation in vacuum, which is the superposition of the incident and reflected pulses, in the following form (see Appendix A)

$$\begin{aligned}\boldsymbol{E}_L(\boldsymbol{r},t) = {}& \frac{1}{2}\boldsymbol{e}_y E_{0L}\frac{2\pi R_x\tau}{\cos\alpha}\int_{-\infty}^{+\infty}\frac{{\rm d}\omega}{2\pi}\exp\left[-{\rm i}\omega t - \frac{(\omega-\omega_0)^2\tau^2}{2}\right]\\ &\times\int_{-\infty}^{+\infty}\frac{{\rm d}k_x}{2\pi}\exp\left\{{\rm i}k_x x - \frac{[k_x-(\omega/c)\sin\alpha]^2R_x^2}{2\cos^2\alpha}\right\}\\ &\times\left\{\exp\left({\rm i}z\sqrt{\frac{\omega^2}{c^2}-k_x^2}\right) + R(\omega,k_x)\exp\left(-{\rm i}z\sqrt{\frac{\omega^2}{c^2}-k_x^2}\right)\right\} + {\rm c.c.}, \quad z\le 0,\end{aligned} \tag{2.2}$$

where $R(\omega, k_x)$ is the Fourier image of the reflection coefficient for s-polarized radiation, which is determined from the boundary conditions. The electric field of the laser pulse in plasma, by analogy with formula (2.2), can also be written in the form of Fourier integrals

$$\begin{aligned}\boldsymbol{E}_L(\boldsymbol{r},t) = {}& \frac{1}{2}\boldsymbol{e}_y E_{0L}\frac{2\pi R_x\tau}{\cos\alpha}\int_{-\infty}^{+\infty}\frac{{\rm d}\omega}{2\pi}\exp\left[-{\rm i}\omega t - \frac{(\omega-\omega_0)^2\tau^2}{2}\right]\\ &\times\int_{-\infty}^{+\infty}\frac{{\rm d}k_x}{2\pi}T(\omega,k_x)\exp\left\{{\rm i}k_x x + {\rm i}z\sqrt{\frac{\omega^2}{c^2}\varepsilon(\omega)-k_x^2} - \frac{[k_x-(\omega/c)\sin\alpha]^2R_x^2}{2\cos^2\alpha}\right\}\\ &+ {\rm c.c.}, \quad z\ge 0,\end{aligned} \tag{2.3}$$

where $T(\omega, k_x)$ is the Fourier image transmission coefficient for the s-polarized wave, $\varepsilon(\omega) = 1 - \omega_p^2/\omega^2$ is the dielectric permittivity of the plasma at the frequency ω. From the continuity conditions for the tangential components of the electric and magnetic fields of laser radiation at the plasma–vacuum interface, we find expressions for the Fourier components of the reflection and transmission coefficients

$$\left.\begin{aligned}R(\omega,k_x) &= \frac{\sqrt{(\omega^2/c^2)-k_x^2}-\sqrt{(\omega^2/c^2)\varepsilon(\omega)-k_x^2}}{\sqrt{(\omega^2/c^2)-k_x^2}+\sqrt{(\omega^2/c^2)\varepsilon(\omega)-k_x^2}},\\ T(\omega,k_x) &= \frac{2\sqrt{(\omega^2/c^2)-k_x^2}}{\sqrt{(\omega^2/c^2)-k_x^2}+\sqrt{(\omega^2/c^2)\varepsilon(\omega)-k_x^2}}.\end{aligned}\right\} \tag{2.4}$$

Let us consider the electric field of laser radiation in plasma near the plasma–vacuum interface, when $z \to +0$. Taking into account the inequalities $\omega_0\tau \gg 1$, $k_0 R_x \gg 1$, from

https://doi.org/10.1017/S0022377822001313 Published online by Cambridge University Press

(2.3) we find the following field distribution near the plasma boundary:

$$\boldsymbol{E}_L(x, z = +0, t) = \boldsymbol{e}_y \frac{2E_{0L}\cos\alpha}{\cos\alpha + \sqrt{\cos^2\alpha - N(\omega_0)}} \times \exp\left[-\frac{1}{2\tau^2}\left(t - \frac{x}{c}\sin\alpha\right)^2 - \frac{x^2}{2R_x^2}\cos^2\alpha\right]\cos\left[\omega_0\left(t - \frac{x}{c}\sin\alpha\right)\right], \tag{2.5}$$

where $N(\omega_0) = \omega_p^2/\omega_0^2 = N_{0e}/N_{\rm cr}$ is the dimensionless electron density. As noted earlier (Frolov 2020), when a laser pulse is incident at the angle of total reflection and the condition

$$\cos^2\alpha = N(\omega_0), \tag{2.6}$$

or $\sin^2\alpha = \varepsilon(\omega_0)$ is fulfilled, the amplitude of the laser radiation electric field in the plasma doubles compared with the amplitude of the incident field in vacuum, as follows from the comparison of (2.1) and (2.5). It should be noted that, when a laser pulse falls on the boundary of very rarefied plasma ($\cos^2\alpha \gg N(\omega_0)$), it crosses the plasma–vacuum interface without reflection (see formula (2.5)) since the electric field of the incident (2.1) and transmitted (2.5) laser pulses coincide in magnitude. However, for an arbitrary finite value of the electron density, there is the certain angle of incidence for which the total reflection of the laser pulse takes place and this angle is determined from relation (2.6). This effect is similar to the effect of total internal reflection of light that falls from an optically denser medium onto the boundary of a medium with a lower refractive index, since vacuum is an optically denser medium (the refractive index is 1) than plasma whose refractive index is less than unity ($\sqrt{\varepsilon(\omega_0)} < 1$). In accordance with formula (2.6), we conclude that the total reflection of laser radiation from rarefied plasma occurs at grazing angles and the lower the electron density, the closer this angle is to $\pi/2$. Thus, the total reflection of a laser pulse from plasma with a sufficiently low electron density occurs when it propagates almost along the boundary. It follows from formula (2.5) that the electric field of laser radiation in plasma near the boundary under condition (2.6) has a value twice as high as the field of the incident laser pulse (2.1). This effect takes place due to the fact that, under the condition of total reflection (2.6), the electric field of laser radiation at the plasma boundary (2.6) is equal to the sum of the incident and reflected fields, which are equal in absolute value.

Using the expression for the electric field (2.5) and the definition of the potential of laser radiation ponderomotive forces $\Phi(\boldsymbol{r}, t)$ acting on plasma electrons

$$\Phi(\boldsymbol{r}, t) = \frac{e}{2m_e}\left\langle\left(\int_{-\infty}^{t} {\rm d}t' \boldsymbol{E}_L(\boldsymbol{r}, t')\right)^2\right\rangle, \tag{2.7}$$

where angle brackets $\langle\cdots\rangle$ mean averaging over the period of high-frequency oscillations $2\pi/\omega_0$, we find the ponderomotive potential $\Phi(\boldsymbol{r}, t)$ near the plasma boundary

$$\Phi(x, z = +0, t) = \frac{eE_{0L}^2}{4m_e\omega_0^2}\left|\frac{2\cos\alpha}{\cos\alpha + \sqrt{\cos^2\alpha - N(\omega_0)}}\right|^2 \times \exp\left\{-\frac{1}{\tau^2}\left[t - \frac{x}{c}\sin\alpha\right]^2 - \frac{x^2}{R_x^2}\cos^2\alpha\right\}, \tag{2.8}$$

which differs from the corresponding expression (14) in (Frolov 2020) by taking into account the transverse size of the laser pulse. The ponderomotive action of laser radiation

https://doi.org/10.1017/S0022377822001313 Published online by Cambridge University Press

with potential (2.8) leads to the excitation of THz fields in the plasma and their emission into vacuum. It should be noted that the ponderomotive effect is significantly enhanced when the laser pulse is incident at the angle of total reflection (2.6), since in this case the potential (2.8) increases by a factor of 4 compared with the case of incidence at smaller angles, when the condition $\cos^2\alpha \gg N(\omega_0)$ is satisfied.

3. Excitation of THz fields in vacuum and plasma

To describe the generation of THz radiation, we will use the time-averaged Maxwell equations for the electric $\boldsymbol{E}(\boldsymbol{r}, t)$ and magnetic $\boldsymbol{B}(\boldsymbol{r}, t)$ fields

$$rot\boldsymbol{B}(\boldsymbol{r}, t) = \frac{1}{c}\frac{\partial}{\partial t}\boldsymbol{E}(\boldsymbol{r}, t) + \frac{4\pi}{c}eN_e(z)\boldsymbol{V}(\boldsymbol{r}, t), \quad rot\boldsymbol{E}(\boldsymbol{r}, t) = -\frac{1}{c}\frac{\partial}{\partial t}\boldsymbol{B}(\boldsymbol{r}, t), \tag{3.1a,b}$$

as well as the equation for the electron velocity $\boldsymbol{V}(\boldsymbol{r}, t)$, taking into account the ponderomotive effect of laser radiation (see, for example, Frolov 2020)

$$\left(\frac{\partial}{\partial t} + \nu_{ei}\right)\boldsymbol{V}(\boldsymbol{r}, t) = \frac{e}{m_e}[\boldsymbol{E}(\boldsymbol{r}, t) - \nabla\Phi(\boldsymbol{r}, t)], \tag{3.2}$$

which is obtained in the non-relativistic approximation $|\boldsymbol{V}(\boldsymbol{r}, t)| \ll c$ under the condition of rare electron collisions $\nu_{ei}\tau \ll 1$, where $N_e(z) = N_{0e}\theta(z)$ is the coordinate-dependent electron density, $\theta(z)$ is the Heaviside unit step function and ν_{ei} is the frequency of electron–ion collisions.

Using a Fourier transform with respect to time and x coordinate from the set of (3.1), (3.2) we find the following equation for the low-frequency magnetic field $B_y(\omega, k_x, z)$:

$$\frac{\mathrm{d}}{\mathrm{d}z}\left\{\frac{1}{\varepsilon(\omega, z)}\frac{\mathrm{d}}{\mathrm{d}z}B_y(\omega, k_x, z)\right\} + \left[\frac{\omega^2}{c^2} - \frac{k_x^2}{\varepsilon(\omega, z)}\right]B_y(\omega, k_x, z)$$
$$= \frac{\omega}{c}k_x\left\{\frac{\omega_p^2(z)}{\omega(\omega + i\nu_{ei})\varepsilon(\omega, z)}\frac{\mathrm{d}}{\mathrm{d}z}\Phi(\omega, k_x, z) - \frac{\mathrm{d}}{\mathrm{d}z}\left[\frac{\omega_p^2(z)\Phi(\omega, k_x, z)}{\omega(\omega + i\nu_{ei})\varepsilon(\omega, z)}\right]\right\}, \tag{3.3}$$

at the same time the components of the electric field $E_x(\omega, k_x, z)$, $E_z(\omega, k_x, z)$, are determined by the following relationships:

$$\left.\begin{aligned} E_x(\omega, k_x, z) &= -\frac{ic}{\omega\varepsilon(\omega, z)}\frac{\mathrm{d}}{\mathrm{d}z}B_y(\omega, k_x, z) - \frac{ik_x\omega_p^2(z)}{\omega(\omega + i\nu_{ei})\varepsilon(\omega, z)}\Phi(\omega, k_x, z) \\ E_z(\omega, k_x, z) &= -\frac{ck_x}{\omega\varepsilon(\omega, z)}B_y(\omega, k_x, z) - \frac{\omega_p^2(z)}{\omega(\omega + i\nu_{ei})\varepsilon(\omega, z)}\frac{\mathrm{d}}{\mathrm{d}z}\Phi(\omega, k_x, z) \end{aligned}\right\}, \tag{3.4}$$

where $\varepsilon(\omega, z) = 1 - \omega_p^2(z)/\omega^2$, $\omega_p^2(z) = 4\pi e^2N_e(z)/m_e$ and $\Phi(\omega, k_x, z)$ is the Fourier image of the ponderomotive potential. The solution of (3.3) for the low-frequency magnetic field in a plasma and in a vacuum, taking into account the boundary conditions of the continuity for $E_x(\omega, k_x, z)$ and $B_y(\omega, k_x, z)$, has the following form:

$$B_y(\omega, k_x, z) = \frac{\mathrm{i}\omega k_x}{c}\frac{\omega_p^2}{\omega(\omega + i\nu_{ei})}\frac{\Phi(\omega, k_x, z = 0)}{D(\omega, k_x)}\exp\left\{-\mathrm{i}z\sqrt{\frac{\omega^2}{c^2} - k_x^2}\right\}, \quad z \le 0, \tag{3.5}$$

$$B_y(\omega, k_x, z) = \frac{\mathrm{i}\omega k_x}{c}\frac{\omega_p^2}{\omega(\omega + i\nu_{ei})}\frac{\Phi(\omega, k_x, z = 0)}{D(\omega, k_x)}\exp\left\{\mathrm{i}z\sqrt{\frac{\omega^2}{c^2}\varepsilon(\omega) - k_x^2}\right\}, \quad z \ge 0, \tag{3.6}$$

https://doi.org/10.1017/S0022377822001313 Published online by Cambridge University Press

where the function $D(\omega, k_x)$ is given by the formula

$$D(\omega, k_x) = \varepsilon(\omega)\sqrt{\frac{\omega^2}{c^2} - k_x^2} + \sqrt{\frac{\omega^2}{c^2}\varepsilon(\omega) - k_x^2}. \tag{3.7}$$

It follows from formulas (3.5), (3.6) that the low-frequency magnetic field in plasma and in vacuum is determined by the Fourier transform of the ponderomotive potential at the plasma boundary $\Phi(\omega, k_x, z = 0)$, which, in accordance with (2.8), has the form

$$\Phi(\omega, k_x, z = 0) = \frac{eE_{0L}^2}{4m_e\omega_0^2}\left|\frac{2\cos\alpha}{\cos\alpha + \sqrt{\cos^2\alpha - N(\omega_0)}}\right|^2 \times \frac{\pi R\tau}{\cos\alpha}\exp\left\{-\frac{\omega^2\tau^2}{4} - \left(k_x - \frac{\omega}{c}\sin\alpha\right)^2\frac{R_x^2}{4\cos^2\alpha}\right\}. \tag{3.8}$$

The obtained expression for the magnetic field (3.5), taking into account formulas (3.7), (3.8), allows us to analyse the characteristics of the THz pulse, which is emitted from the plasma into vacuum.

4. Spectral, angular and energy characteristics of THz radiation in vacuum

Using the inverse Fourier transform with respect to the spatial coordinate from formula (3.5), we find the THz magnetic field in vacuum

$$B_y(\omega, \boldsymbol{r}) = \frac{\omega_p^2}{c(\omega + i\nu_{ei})}\frac{\partial}{\partial x}\int_{-\infty}^{+\infty}\frac{\mathrm{d}k_x}{2\pi}\exp\left\{\mathrm{i}k_x x - \mathrm{i}z\sqrt{\frac{\omega^2}{c^2} - k_x^2}\right\}\frac{\Phi(\omega, k_x, z = 0)}{D(\omega, k_x)}, \quad z \le 0. \tag{4.1}$$

We will consider the field (4.1), (3.8) at large distances from the plasma boundary in the wave zone, when the condition $r = \sqrt{x^2 + z^2} \gg L, R, c/\omega$ is satisfied. In this case, the integral in formula (4.1) can be calculated using the stationary phase method (Olver 1974). For large values of the exponential function argument, the main contribution to the integral is made by the small neighbourhood near the stationary point, the position of which is determined by the formula

$$k_{x,s} = \frac{\omega}{c}\sin\theta, \tag{4.2}$$

where θ is the angle between the direction of observation and the positive direction of the z axis. The position of the stationary point (4.2) is found from the condition that the derivative of the argument of the exponential function in formula (4.1) is equal to zero. Calculating the integral in formula (4.1) taking into account the contribution of the stationary point (4.2) for the Fourier transform of the THz magnetic field in vacuum, we obtain the following expression:

$$B_y(\omega, \boldsymbol{r}) = \frac{\omega_p^2}{\omega_0(\omega + i\nu_{ei})}\frac{V_E}{4c}E_{0L}\frac{\pi R_x\tau}{\cos\alpha}\left|\frac{2\cos\alpha}{\sin\alpha + \sqrt{\cos^2\alpha - N(\omega_0)}}\right|^2\sqrt{\frac{\omega}{2\pi rc}} \times \frac{\sin\theta|\cos\theta|}{\varepsilon(\omega)|\cos\theta| + \sqrt{\varepsilon(\omega) - \sin^2\theta}} \times \exp\left\{\mathrm{i}\frac{\pi}{4} + \mathrm{i}\frac{\omega}{c}r - \frac{\omega^2\tau^2}{4} - \left(\frac{\sin\theta - \sin\alpha}{\cos\alpha}\right)^2\frac{\omega^2R_x^2}{4c^2}\right\}, \quad z \le 0, \tag{4.3}$$

https://doi.org/10.1017/S0022377822001313 Published online by Cambridge University Press

where $V_E = eE_{0L}/(m_e\omega_0)$ is the amplitude of the electron oscillation velocity in the laser field (2.1). Using formula (4.3), we find the energy that is radiated into the unit frequency interval $\mathrm{d}\omega$ and is carried through the unit cylindrical area $\mathrm{d}\boldsymbol{f} = \boldsymbol{e}_r r\,\mathrm{d}\theta\,\mathrm{d}y$ along the normal to it

$$\mathrm{d}W(\omega,\theta) = \frac{c}{8\pi^2}\{[\boldsymbol{E}(\omega,\boldsymbol{r})\times\boldsymbol{B}^*(\omega,\boldsymbol{r})] + \mathrm{c.c.}\}\,\mathrm{d}\omega\,\mathrm{d}\boldsymbol{f} = \frac{c}{4\pi^2}|B_y(\omega,\boldsymbol{r})|^2 r\,\mathrm{d}\theta\,\mathrm{d}y\,\mathrm{d}\omega. \tag{4.4}$$

Taking into account formulas (4.3), (4.4), we find the energy radiated in the unit interval of frequencies $\mathrm{d}\omega$ and angles $\mathrm{d}\theta$

$$\begin{aligned}\frac{\mathrm{d}W(\omega,\theta)}{\mathrm{d}\omega\,\mathrm{d}\theta} = {}& \frac{\omega_p^2}{\omega_0^2}\frac{\omega_p\tau k_p R_x\omega}{\omega^2+\nu_{ei}^2}\frac{V_E^2}{c^2}\frac{W_L}{\pi}\frac{\cos^2\alpha}{|\cos\alpha+\sqrt{\cos^2\alpha-N(\omega_0)}|^4}\\ &\times\frac{\sin^2\theta\cos^2\theta}{\left|\varepsilon(\omega)|\cos\theta|+\sqrt{\varepsilon(\omega)-\sin^2\theta}\right|^2}\\ &\times\exp\left\{-\frac{\omega^2\tau^2}{2}\left[1+\frac{R_x^2}{L^2}\left(\frac{\sin\theta-\sin\alpha}{\cos\alpha}\right)^2\right]\right\},\quad z\le 0,\end{aligned} \tag{4.5}$$

where $W_L = E_{0L}^2 R_x R_y L/8$ is the energy of the laser pulse, R_y is the size of the laser pulse along the y axis and $k_p = \omega_p/c$. If we integrate over frequencies in formula (4.5), then we find the THz radiation pattern

$$\begin{aligned}\frac{\mathrm{d}W(\theta)}{\mathrm{d}\theta} = {}& \frac{R_x}{L}\frac{V_E^2}{c^2}\frac{W_L}{\pi}J(\theta),\\ J(\theta) = {}& \frac{\omega_0^2\tau^2N^2(\omega_0)\sin^2\theta\cos^2\theta\cos^2\alpha}{|\cos\alpha+\sqrt{\cos^2\alpha-N(\omega_0)}|^4}\\ &\times\int_0^\infty\frac{\mathrm{d}\Omega\,\Omega^3}{|(\Omega^2-1)|\cos\theta|+\Omega\sqrt{\Omega^2\cos^2\theta-1}|^2}\\ &\times\exp\left\{-\frac{N(\omega_0)\omega_0^2\tau^2\Omega^2}{2}\left[1+\frac{R_x^2}{L^2}\left(\frac{\sin\theta-\sin\alpha}{\cos\alpha}\right)^2\right]\right\}.\end{aligned} \tag{4.6}$$

The spectrum of THz radiation is calculated by integrating in formula (4.5) over the angles

$$\begin{aligned}\frac{\mathrm{d}W(\Omega)}{\mathrm{d}\Omega} = {}& \frac{R_x}{L}\frac{V_E^2}{c^2}\frac{W_L}{\pi}I(\Omega),\\ I(\Omega) = {}& \frac{\omega_0^2\tau^2N^2(\omega_0)\cos^2\alpha}{|\cos\alpha+\sqrt{\cos^2\alpha-N(\omega_0)}|^4}\Omega^3\\ &\times\int_{\pi/2}^{3\pi/2}\frac{\mathrm{d}\theta\sin^2\theta\cos^2\theta}{|(\Omega^2-1)|\cos\theta|+\Omega\sqrt{\Omega^2\cos^2\theta-1}|^2}\\ &\times\exp\left\{-\frac{N(\omega_0)\omega_0^2\tau^2\Omega^2}{2}\left[1+\frac{R_x^2}{L^2}\left(\frac{\sin\theta-\sin\alpha}{\cos\alpha}\right)^2\right]\right\},\end{aligned} \tag{4.7}$$

https://doi.org/10.1017/S0022377822001313 Published online by Cambridge University Press

where $\Omega = \omega/\omega_p$ is the dimensionless frequency. The total energy of THz radiation can be calculated by integrating over angles in formula (4.6) or over frequencies in formula (4.7)

$$W = \frac{R_x}{L}\frac{V_E^2}{c^2}\frac{W_L}{\pi}w, \quad w = \frac{\omega_0^2\tau^2 N^2(\omega_0)\cos^2\alpha}{|\cos\alpha + \sqrt{\cos^2\alpha - N(\omega_0)}|^4}\int_{\pi/2}^{3\pi/2} d\theta \sin^2\theta\cos^2\theta \times \int_0^\infty \frac{d\Omega\,\Omega^3}{|(\Omega^2-1)|\cos\theta| + \Omega\sqrt{\Omega^2\cos^2\theta - 1}|^2} \times \exp\left\{-\frac{N(\omega_0)\omega_0^2\tau^2\Omega^2}{2}\left[1 + \frac{R_x^2}{L^2}\left(\frac{\sin\theta - \sin\alpha}{\cos\alpha}\right)^2\right]\right\}. \tag{4.8}$$

We will further assume that the laser pulse energy, its wavelength and duration are fixed values, whereas the size of the focal spot and radiation intensity (these parameters are determined by the degree of focusing), as well as the angle of incidence are variable. The electron density of the plasma can also be a variable, which is determined by the type of target irradiated by the laser.

The total energy of THz radiation (4.8) as a function of the incidence angle for different degrees of laser radiation focusing is shown in figure 1. It follows from figure 1 that the total energy of THz radiation is maximum when the laser pulse is grazingly incident at the angle of total reflection (2.6) onto a rarefied plasma whose density for the indicated parameters is almost three orders of magnitude less than the critical value. Also, the energy of the THz pulse increases with a decrease in the size of the laser radiation focal spot. If condition (2.6) is satisfied and the laser pulse is incident at the angle of total reflection, then the maximum value of the total energy of THz radiation (4.8) takes the form

$$W_{\max} = \frac{R_x}{L}\frac{V_E^2}{c^2}\frac{W_L}{\pi}w_{\max}, \quad w_{\max} = N(\omega_0)\omega_0^2\tau^2\int_{\pi/2}^{3\pi/2} d\theta \sin^2\theta\cos^2\theta \times \int_0^\infty \frac{d\Omega\,\Omega^3}{|(\Omega^2-1)|\cos\theta| + \Omega\sqrt{\Omega^2\cos^2\theta - 1}|^2} \times \exp\left\{-\frac{N(\omega_0)\omega_0^2\tau^2\Omega^2}{2}\left[1 + \frac{R_x^2}{L^2}\left(\frac{\sin\theta - \sqrt{1-N(\omega_0)}}{\sqrt{N(\omega_0)}}\right)^2\right]\right\}. \tag{4.9}$$

It follows from formula (4.9) that the dimensionless energy has the maximum value

$$w_{\max}(R_x \to 0) = \omega_p^2\tau^2\int_{\pi/2}^{3\pi/2} d\theta \sin^2\theta\cos^2\theta \int_0^\infty \frac{d\Omega\,\Omega^3\exp\{-\omega_p^2\tau^2\Omega^2/2\}}{|(\Omega^2-1)|\cos\theta| + \Omega\sqrt{\Omega^2\cos^2\theta - 1}|^2}, \tag{4.10}$$

in the limit $R_x \to 0$, that is, for tight focusing of the laser pulse. In this case, it should be taken into account that the minimum value of the focal spot size is limited by the wavelength of laser radiation λ_0. The dimensionless energy of THz radiation for the laser pulse for extremely tight focusing (4.10) as a function of the plasma density is shown in figure 2.

For the duration of the laser pulse $\tau = 100/\omega_0$, the energy is maximum for the density $N_{0e} \approx 1.6 \times 10^{-4} N_{\rm cr}$, which corresponds to the parameter $\omega_p\tau \approx 1.3$. The energy of THz radiation (4.9) for the indicated value of the electron density as a function of the focal spot size is shown in figure 3, from which it follows that the THz energy noticeably increases

https://doi.org/10.1017/S0022377822001313 Published online by Cambridge University Press

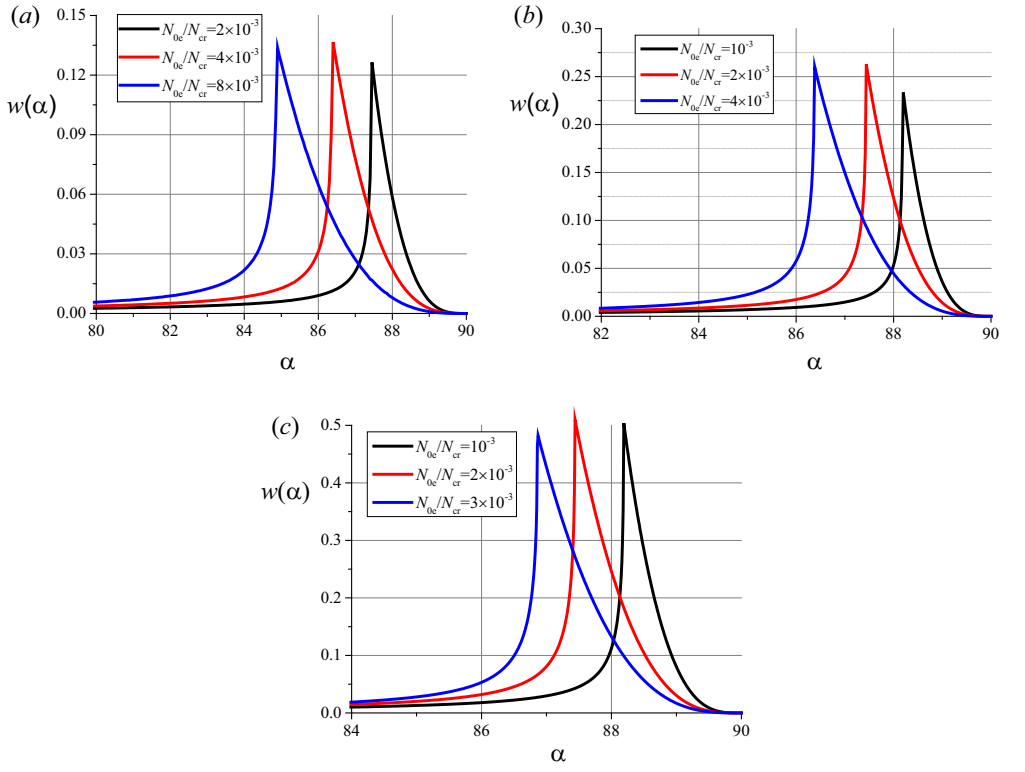

FIGURE 1. The THz radiation energy (4.8) as a function of the laser pulse incidence angle at $\omega_0\tau = 100$ for different electron densities and for $(R_x/L)^2 = 4$ (a), $(R_x/L)^2 = 1$ (b), $(R_x/L)^2 = 0.25$ (c).

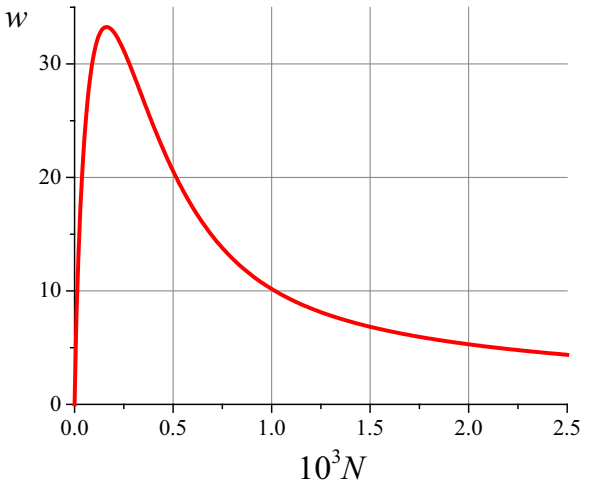

FIGURE 2. The energy of THz radiation as the function of the electron density (4.10) when the tight focused ($R_x \to 0$) laser pulse is incident at the angle of total reflection (2.6) at $\omega_0\tau = 100$.

with a decrease in the focal spot size of the laser pulse. If at $R_x = L$ the dimensionless energy of THz radiation is $w \approx 0.12$, then with a decrease in the size of the laser pulse focal spot, a sharp increase in the energy of THz radiation takes place, and at the extremely

https://doi.org/10.1017/S0022377822001313 Published online by Cambridge University Press

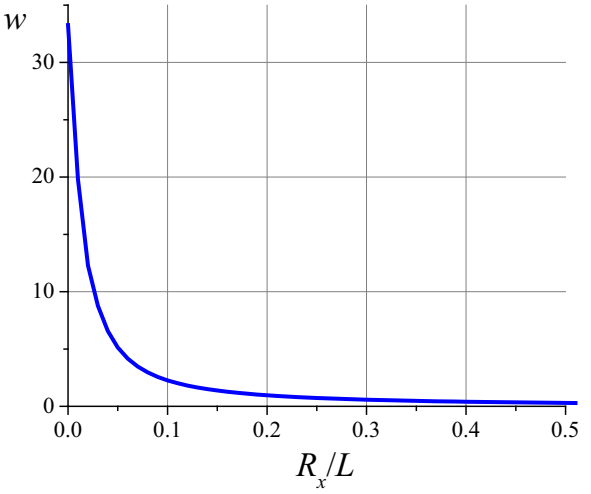

FIGURE 3. The energy of THz radiation (4.9) as the function of the degree of laser pulse focusing when it is incident at the angle of total reflection (2.6), at $\omega_0\tau = 100$, $N_{0e} = 1.6 \times 10^{-4} N_{\rm cr}$.

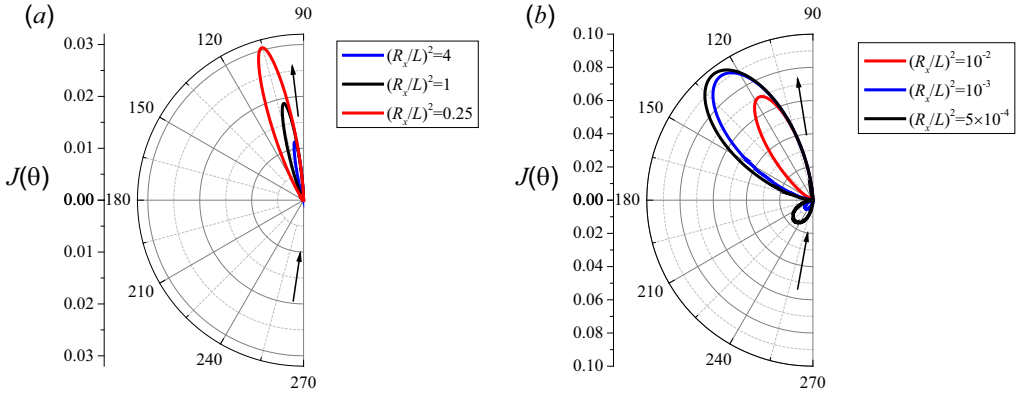

FIGURE 4. The THz radiation pattern for the incidence of the laser pulse with duration $\tau = 100/\omega_0$ at the angle of total reflection (2.6) on the plasma with the electron density $N_{0e} = 10^{-3} N_{\rm cr}$ at various degrees of focusing. The arrows show the direction of propagation of the incident and reflected laser pulses.

tight focusing $R_x \to 0$, THz energy reaches the value $w \approx 33$, which is more than two orders of magnitude greater than at $R_x = L$.

The THz radiation pattern (4.6) is shown in figure 4. At large sizes of the laser pulse focal spot, THz waves are emitted in the direction approximately coinciding with the direction of the reflected laser pulse propagation (see figure 4*a*).

This result follows from formula (4.6) under the condition $R_x \gg L$ and was previously presented for an unfocused laser pulse ($R_x \to \infty$) in a number of publications (see, for example, Frolov 2020, 2021). A decrease in the size of the laser pulse focal spot leads to the fact that the radiation pattern of THz radiation becomes wider and shifts towards the normal to the plasma boundary. The case of extremely tight focusing of laser radiation

https://doi.org/10.1017/S0022377822001313 Published online by Cambridge University Press

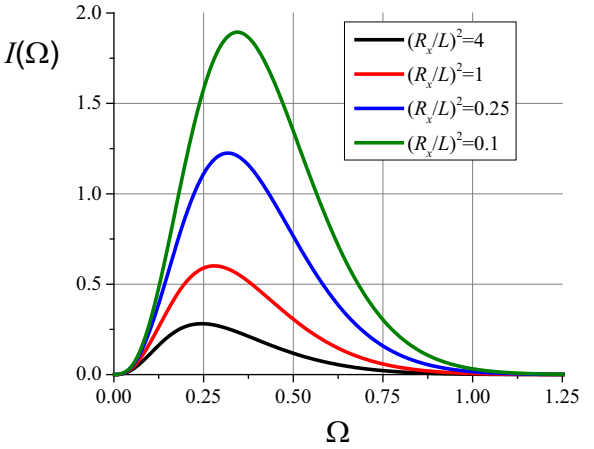

FIGURE 5. The spectrum of THz radiation when a laser pulse with duration $\tau = 100/\omega_0$ is incident at the angle of total reflection (2.6) onto the plasma with the electron density $N_{0e} = 10^{-3}N_{\rm cr}$ at various degrees of focusing.

is shown in figure 4(*b*). In this case, radiation with lower energy appears in the specular direction in the range of angles $\pi \leq \theta \leq 3\pi/2$.

The energy of THz radiation as a function of frequency (4.7) is shown in figure 5 for different degrees of the laser radiation focusing.

A decrease in the size of the focal spot leads to an increase in the height of the spectral line and its shift to the region of higher frequencies. If, for a large transverse dimension of the laser pulse, the maximum in the THz radiation spectrum corresponds to a frequency of the order of the reciprocal duration $\omega_{\max} \approx 1/\tau$, which is less than the plasma frequency, then, with a decrease in the transverse dimension, the frequency approaches the plasma frequency and can become equal to it.

5. Conclusion

In this article, we consider the generation of THz radiation at oblique incidence of a focused *s*-polarized laser pulse on semi-bounded rarefied plasma. The boundary value problem for laser radiation is solved and the laser field and the ponderomotive potential in the plasma near its boundary are found. Based on the Maxwell equations averaged over the laser period and the equation for the electron velocity, which takes into account the ponderomotive effect of laser radiation, the excitation of THz fields in plasma and their emission into vacuum are considered. The energy, angular and spectral characteristics of THz radiation in vacuum are studied as functions of the incidence angle and the focusing degree of the laser pulse, as well as the plasma density. It is shown that the energy of the THz signal noticeably increases with a decrease in the size of the focal spot, and the THz energy reaches the maximum at tight focusing of laser radiation, when it is incident at the angle of total reflection on the plasma boundary. The THz radiation pattern is studied as a function of the focal spot size of the laser pulse. It is shown that, as the transverse size of the laser radiation decreases, the THz signal pattern shifts from the grazing angle, which coincides with the direction of the reflected laser pulse, towards the normal to the plasma–vacuum interface. It has been established that, for extremely tight focusing of the laser pulse, an additional THz radiation signal with a lower energy appears which propagates with respect to the main signal in the mirror direction relative to the

https://doi.org/10.1017/S0022377822001313 Published online by Cambridge University Press

normal to the plasma boundary. The frequency dependence of the THz radiation energy is considered and it is shown that, as the focal spot size decreases, the maximum in the emission spectrum increases, and its position shifts to higher frequencies and can approach to the plasma frequency.

In the considered model, the plasma boundary is assumed to be sharp, which enabled us to formulate the corresponding boundary conditions for calculating the fields and thereby to substantially simplify the problem. It can be assumed that the theory of THz wave generation developed in the article is applicable if the characteristic scale of the plasma–vacuum transition layer L_p is smaller than the sizes of the laser pulse L, R_x and the plasma wavelength $2\pi c/\omega_p$.

In conclusion, we present estimates for the characteristics of THz radiation for typical parameters of modern laser-plasma experiments. Let a laser pulse with wavelength $\lambda_0 = 1.24\ \mu\text{m}$ (frequency $\omega_0 \approx 1.52 \times 10^{15} c^{-1}$), duration $\tau = 66$ fs, energy $W_L = 600$ mJ and transverse dimensions $R_x = 3\ \mu\text{m}$, $R_y = 0.1$ cm (for these parameters, the power and intensity of the laser pulse are equal to $P_L \approx 3.5$ TW, $I_L \approx 10^{17}$ W cm^{-2}) be incident at the angle $\alpha = 89^\circ$ onto the boundary of a fully ionized plasma whose electrons have density $N_{0e} = 1.2 \times 10^{17}$ cm^{-3}, which is much less than the critical value 0.7×10^{21} cm^{-3}, then, in this case, the radiation of THz waves at the frequency $\nu_{\text{THz}} \approx 0.3\omega_p/(2\pi) \approx 0.9$ THz, which corresponds to the wavelength $\lambda_{\text{THz}} \approx 330\ \mu\text{m}$, occurs at the angle $\theta \approx 110^\circ$, which corresponds to the angle 70° relative to the normal to the plasma–vacuum interface. In accordance with formula (4.9), the energy of the THz radiation is equal to $W_{\text{THz}} \approx 0.74 \times 10^{-2} W_L \approx 4.6$ mJ and is approximately a per cent of the laser pulse energy. If the duration of the THz signal is comparable to the duration of the laser pulse, then for the THz radiation power we have the following estimate: $P_{\text{THz}} \approx 0.74 \times 10^{-2} P_L \approx 26$ GW. These estimates indicate the possibility of generating high-power THz pulses under the action of tightly focused s-polarized laser radiation at its grazing incidence on a rarefied plasma boundary, when the effect of total reflection takes place.

Acknowledgements

Editor Victor Malka thanks the referees for their advice in evaluating this article.

Declaration of interests

The author reports no conflict of interest.

Appendix A. Boundary value problem for s-polarized laser pulse

To solve the boundary value problem when the s-polarized laser pulse (2.1) is incident on a semi-bounded plasma, we will use the Maxwell equations

$$\left.\begin{aligned} rot\boldsymbol{E}_L(\boldsymbol{r},t) &= -\frac{1}{c}\frac{\partial}{\partial t}\boldsymbol{B}_L(\boldsymbol{r},t), \\ rot\boldsymbol{B}_L(\boldsymbol{r},t) &= \frac{1}{c}\frac{\partial}{\partial t}\boldsymbol{E}_L(\boldsymbol{r},t) + \frac{4\pi e}{c}N_{0e}\boldsymbol{V}_L(\boldsymbol{r},t), \end{aligned}\right\} \tag{A1}$$

where $\boldsymbol{E}_L(\boldsymbol{r},t)$, $\boldsymbol{B}_L(\boldsymbol{r},t)$ are the electric and magnetic fields of laser radiation, and the electron velocity $\boldsymbol{V}_L(\boldsymbol{r},t)$ satisfies the equation

$$\frac{\partial}{\partial t}\boldsymbol{V}_L(\boldsymbol{r},t) = \frac{e}{m_e}\boldsymbol{E}_L(\boldsymbol{r},t). \tag{A2}$$

https://doi.org/10.1017/S0022377822001313 Published online by Cambridge University Press

From the set of (A1), (A2) we find the equation for the y-component of the laser pulse electric field $E_L(\boldsymbol{r}, t) = \boldsymbol{e}_y \cdot \boldsymbol{E}_L(\boldsymbol{r}, t)$

$$\frac{\partial^2}{\partial t^2} E_L(\boldsymbol{r}, t) + \omega_p^2 E_L(\boldsymbol{r}, t) - c^2 \Delta E_L(\boldsymbol{r}, t) = 0, \tag{A3}$$

where Δ is the Laplace operator.

To solve (A3), we will use the Fourier transform in time and coordinate

$$\left.\begin{aligned} E_L(\boldsymbol{r}, t) &= \int_{-\infty}^{+\infty} \frac{\mathrm{d}\omega}{2\pi} \int_{-\infty}^{+\infty} \frac{\mathrm{d}k_x}{2\pi} \exp(-\mathrm{i}\omega t + \mathrm{i}k_x x) E_L(\omega, k_x, z), \\ E_L(\omega, k_x, z) &= \int_{-\infty}^{+\infty} \mathrm{d}t \int_{-\infty}^{+\infty} \mathrm{d}x \exp(\mathrm{i}\omega t - \mathrm{i}k_x x) E_L(\boldsymbol{r}, t). \end{aligned}\right\} \tag{A4}$$

Then from (A3) the ordinary differential equation for the Fourier transform of the electric field follows

$$\frac{\mathrm{d}^2}{\mathrm{d}z^2} E_L(\omega, k_x, z) + \left[\frac{\omega^2}{c^2}\varepsilon(\omega) - k_x^2\right] E_L(\omega, k_x, z) = 0, \tag{A5}$$

whose solution, taking into account the continuity of the tangential components of the field $E_L(\omega, k_x, z)$ and $B_{L,x}(\omega, k_x, z) = (ic/\omega)\,\mathrm{d}E_L(\omega, k_x, z)/\mathrm{d}z$, has the form

$$\left.\begin{aligned} E_L(\omega, k_x, z) = E_0(\omega, k_x) &\left\{ \exp\left(\mathrm{i}z\sqrt{\frac{\omega^2}{c^2} - k_x^2}\right) \right. \\ &\left. + R(\omega, k_x) \exp\left(-\mathrm{i}z\sqrt{\frac{\omega^2}{c^2} - k_x^2}\right) \right\}, \quad z \le 0, \\ E_L(\omega, k_x, z) = E_0(\omega, k_x) T(\omega, k_x) &\exp\left(\mathrm{i}z\sqrt{k_x^2 - \frac{\omega^2}{c^2}\varepsilon(\omega)}\right), \quad z \ge 0, \end{aligned}\right\} \tag{A6}$$

where $\varepsilon(\omega)$ is the plasma permittivity, and the reflection $R(\omega, k_x)$ and transmission $T(\omega, k_x)$ coefficients for an s-polarized wave have the form

$$\left.\begin{aligned} R(\omega, k_x) &= \frac{\sqrt{(\omega^2/c^2) - k_x^2} - \sqrt{(\omega^2/c^2)\varepsilon(\omega) - k_x^2}}{\sqrt{(\omega^2/c^2) - k_x^2} + \sqrt{(\omega^2/c^2)\varepsilon(\omega) - k_x^2}}, \\ T(\omega, k_x) &= \frac{2\sqrt{(\omega^2/c^2) - k_x^2}}{\sqrt{(\omega^2/c^2) - k_x^2} + \sqrt{(\omega^2/c^2)\varepsilon(\omega) - k_x^2}}. \end{aligned}\right\} \tag{A7}$$

To find $E_0(\omega, k_x)$ it is necessary that the expression $E_0(\omega, k_x)\exp\{\mathrm{i}z\sqrt{(\omega^2/c^2) - k_x^2}\}$ from (A6) equates to the Fourier transform of the incident pulse (2.1) near the plasma boundary $z = 0$. As the result, for $E_0(\omega, k_x)$ we obtain the following formula:

$$\begin{aligned} E_0(\omega, k_x) = E_L^{\mathrm{inc}}(\omega, k_x, z = 0) = \frac{E_{0L}\pi R_x \tau}{\cos\alpha} &\left\{ \exp\left[-\frac{(\omega - \omega_0)^2\tau^2}{2}\right] \right. \\ &\left. + \exp\left[-\frac{(\omega + \omega_0)^2\tau^2}{2}\right] \right\} \exp\left\{-\frac{(k_x - (\omega/c)\sin\alpha)^2 R_x^2}{2\cos^2\alpha}\right\}. \end{aligned} \tag{A8}$$

Substituting formula (A8) into (A6) and using the inverse Fourier transform from (A4), we find expressions (2.2)–(2.4) for the electric field of s-polarized laser radiation in vacuum and plasma.

https://doi.org/10.1017/S0022377822001313 Published online by Cambridge University Press

REFERENCES

DECHARD, J., DAVOINE, X., GREMILLET, L. & BERG, L. 2020 Terahertz emission from submicron solid targets irradiated by ultraintense femtosecond laser pulses. *Phys. Plasmas* **27** (9), 093105.

DECHARD, J., DEBAYLE, A., DAVOINE, X., GREMILLET, L. & BERG, L. 2018 Terahertz pulse generation in underdense relativistic plasmas: from photoionization-induced radiation to coherent transition radiation. *Phys. Rev. Lett*. **120** (14), 144801.

DONG, X.G., SHENG, Z.M., WU, H.C., WANG, W.M. & ZHANG, J. 2009 Single-cycle strong terahertz pulse generation from a vacuum-plasma interface driven by intense laser pulses. *Phys. Rev.* E **79** (4), 046411.

DORRANIAN, D., STARODUBTSEV, M., KAWAKAMI, H., ITO, H., YUGAMI, N. & NISHIDA, Y. 2003 Radiation from high-intensity ultrashort-laser-pulse and gas-jet magnetized plasma interaction. *Phys. Rev.* E **68** (2), 026409.

FROLOV, A.A. 2007 Generation of terahertz radiation in the reflection of a laser pulse from a dense plasma. *Plasma Phys. Rep*. **33** (12), 1014–1022.

FROLOV, A.A. 2018 Dipole mechanism generation of terahertz waves under laser–cluster interaction. *Plasma Phys. Rep*. **44** (1), 40–54.

FROLOV, A.A. 2020 Terahertz wave emission at an oblique incidence of the laser pulse on rarefied plasma. *Plasma Phys. Control. Fusion* **62** (9), 0950020.

FROLOV, A.A. 2021 Terahertz emission at a *p*-polarized laser radiation action on plasma. *Phys. Plasmas* **28** (1), 013104.

FÜLÖP, J.A., OLLMANN, Z., LOMBOSI, C., SKROBOL, C., KLINGEBIEL, S., PÁLFALVI, L., KRAUSZ, F., KARSCH, S. & HEBLING, J. 2014 Efficient generation of THz pulses with 0.4 mJ energy. *Opt. Express* **22** (17), 20155–20163.

GOPAL, A., HERZER, S., SCHMIDT, A., SINGH, P., REINHARD, A., ZIEGLER, W., BROMMEL, D., KARMAKAR, A., GIBBON, P., DILLNER, U., MAY, T., MEYER, H.-G. & PAULUS, G.G. 2013 Observation of gigawatt-class THz pulses from a compact laser-driven particle accelerator. *Phys. Rev. Lett*. **111** (7), 074802.

GORBUNOV, L.M. & FROLOV, A.A. 1996 Emission of low-frequency electromagnetic waves by a short laser pulse in stratified rarefied plasma. *J. Expl Theor. Phys*. **83** (5), 967–973.

GORBUNOV, L.M. & FROLOV, A.A. 2004 Electromagnetic radiation at twice the plasma frequency emitted from the region of interaction of two short laser pulses in a rarefied plasma. *J. Expl Theor. Phys*. **98** (3), 527–537.

GORBUNOV, L.M. & FROLOV, A.A. 2006 Low-frequency transition radiation from a short laser pulse at the plasma boundary. *J. Expl Theor. Phys*. **102** (6), 894–901.

HAMSTER, H., SULLIVAN, A., GORDON, S., WHITE, W. & FALCONE, R.W. 1993 Subpicosecond, electromagnetic pulses from intense laser-plasma interaction. *Phys. Rev. Lett*. **71** (17), 2725–2728.

HUANG, S.W., GRANADOS, E., HUANG, W.R., HONG, K.H., ZAPATA, L.E. & KÄRTNER, F.X. 2013 High conversion efficiency, high energy terahertz pulses by optical rectification in cryogenically cooled lithium niobate. *Opt. Lett*. **38** (5), 796–798.

JAHANGIRI, F., HASHIDA, M., NAGASHIMA, T., TOKITA, S., HANGYO, M. & SAKABE, S. 2011 Intense terahertz emission from atomic cluster plasma produced by intense femtosecond laser pulses. *Appl. Phys. Lett*. **99** (26), 261503.

KADLEC, F., KUZEL, P. & COUTAZ, J.-L. 2004 Optical rectification at metal surfaces. *Opt. Lett*. **29** (22), 2674–2676.

KADLEC, F., KUZEL, P. & COUTAZ, J.-L. 2005 Study of terahertz radiation generated by optical rectification on thin gold films. *Opt. Lett*. **30** (11), 1402–1404.

LIAO, G.-Q. & LI, Y.-T. 2019 Review of intense terahertz radiation from relativistic laser-produced plasmas. *IEEE Trans. Plasma Sci*. **47** (6), 3002–3008.

NAGASHIMA, T., HIRAYAMA, H., SHIBUYA, K., HANGYO, M., HASHIDA, M., TOKITA, S. & SAKABE, S. 2009 Terahertz pulse radiation from argon clusters irradiated with intense femtosecond laser pulses. *Opt. Express* **17** (11), 8807–8812.

OH, T.I., YOU, Y.S., JHAJJ, N., ROSENTHAL, E.W., MILCHBERG, H.M. & KIM, K.Y. 2013 Intense terahertz generation in two-color laser filamentation: energy scaling with terawatt laser systems. *New J. Phys*. **15** (7), 075002.

OLVER, F.W.J. 1974 *Asymptotics and Special Functions*. Academic Press.

SCHROEDER, C.B., ESAREY, E., VAN TILBORG, J. & LEEMANS, W.P. 2004 Theory of coherent transition radiation generated at a plasma-vacuum interface. *Phys. Rev.* E **69** (1), 016501.

SHENG, Z.-M., MIMA, K., ZHANG, J. & SANUKI, H. 2005 Emission of electromagnetic pulses from laser wakefields through linear mode conversion. *Phys. Rev. Lett*. **94** (9), 095003.

SONG, H. & NAGATSUMA, T. 2015 *Handbook of Terahertz Technologies: Devices and Applications*. Jenny Stanford Publishing.

SPRANGLE, P., PENANO, J.R., HAFIZI, B. & KAPETANAKOS, C.A. 2004 Ultrashort laser pulses and electromagnetic pulse generation in air and on dielectric surfaces. *Phys. Rev.* E **69** (6), 066415.

SUVOROV, E.V., AKHMEDZHANOV, R.A., FADEEV, D.A., ILYAKOV, I.F., MIRONOV, V.A. & SHISHKIN, B.V. 2012 Terahertz emission from a metallic surface induced by a femtosecond optic pulse. *Opt. Lett*. **37** (13), 2520–2522.

VAN TILBORG, J., SCHROEDER, C.B., FILIP, C.V., TOTH, C., GEDDES, G.R., FUBIANI, G., HUBER, R., KAINDL, R.A., ESAREY, E. & LEEMANS, W.P. 2006 Temporal characterization of femtosecond laser-plasma-accelerated electron bunches using terahertz radiation. *Phys. Rev. Lett*. **96** (1), 014801.

URUPIN, S.A. & FROLOV, A.A. 2012 Generation of low-frequency radiation by dense hot plasma under pondermotive action of a short laser pulse. *J. Expl Theor. Phys*. **114** (5), 878–891.

VICARIO, C., JAZINSEK, M., OVCHINNIKOV, A.V., CHEFONOV, O.V., ASHITKOV, S.I., AGRANAT, M.B. & HAURI, C.P. 2015 High efficiency THz generation in DSTMS, DAST and OH1 pumped by Cr: forsterite laser. *Opt. Express* **23** (4), 4573–4580.

VICARIO, C., OVCHINNIKOV, A.V., ASHITKOV, S.I., AGRANAT, M.B., FORTOV, V.E. & HAURI, C.P. 2014 Generation of 0.9-mJ THz pulses in DSTMS pumped by a Cr:Mg_2SiO_4 laser. *Opt. Lett*. **39** (23), 6632–6635.

WEISS, C., WALLENSTEIN, R. & BEIGANG, R. 2000 Magnetic-field-enhanced generation of terahertz radiation in semiconductor surfaces. *Appl. Phys. Lett*. **77** (25), 4160–4162.

WELSH, G.H. & WYNNE, K. 2009 Generation of ultrafast terahertz radiation pulses on metallic nanostructured surfaces. *Opt. Express* **17** (4), 2470–2480.

YOSHII, J., LAI, C.H., KATSOULEAS, T., JOSHI, C. & MORI, W.B. 1997 Radiation from Cerenkov wakes in a magnetized plasma. *Phys. Rev. Lett*. **79** (21), 4194–4197.

YUGAMI, N., HIGASHIGUCHI, T., GAO, H., SAKAI, S., TAKAHASHI, K., ITO, H., NISHIDA, Y. & KATSOULEAS, T. 2002 Experimental observation of radiation from Cherenkov wakes in a magnetized plasma. *Phys. Rev. Lett*. **89** (6), 065003.

https://doi.org/10.1017/S0022377822001313 Published online by Cambridge University Press